Supporting Information

Morphology-Induced Defects Enhance Lipid Transfer Rates

Yan Xia[1], *Kamil Charubin*[1], *Drew Marquardt*[2,3], *Frederick A. Heberle*[4,5], *John Katsaras*[4,5], *Jianhui Tian*[6], *Xiaolin Cheng*[6], *Ying Liu*[1], *Mu-Ping Nieh**[1,7,8]

[1]Department of Chemical and Biomolecular Engineering, University of Connecticut, Storrs, CT 06269, USA

[2]Institute of Molecular Biosciences, Biophysics Division, NAWI Graz, University of Graz, Graz, 8010, Austria

[3]Department of Physics, Brock University, St. Catharines, Ontario, Canada

[4]Biology and Soft Matter Division, Neutron Sciences Directorate, Oak Ridge National Laboratory, Oak Ridge, TN 37831, USA

[5]Joint Institute for Neutron Sciences, Oak Ridge National Laboratory, Oak Ridge, TN 37831, USA

[6]Center for Molecular Biophysics, Oak Ridge National Laboratory, TN 37831, USA

[7]Polymer Program, Institute of Materials Science, University of Connecticut, Storrs, CT 06269, USA

[8]Department of Biomedical Engineering, University of Connecticut, Storrs, CT 06269, USA

S1 Contrast matched solvents

Neutron scattering length densities (NSLDs) of contrast-matched (CM) solvents are calculated based on the initial equal molar mixtures of *h*- and *d*- bicelles (i.e., $\rho_{CM} = \frac{\rho_{h-Bic}+\rho_{d-Bic}}{2}$ ("Bic" refers to bicelle), where ρ_{CM}, $\rho_{h\text{-}Bic}$ and $\rho_{d\text{-}Bic}$ are the NSLDs of CM solvent bicelles containing protiated and deuterated DPPC, respectively). The molar ratios of H_2O to D_2O are determined by the calculated ρ_{CM}, based on $\rho_{H_2O} = -5.8 \times 10^{-7}$ Å^{-2} and $\rho_{D_2O} = 6.38 \times 10^{-6}$ Å^{-2}. Table S1 tabulates the CM water for each case.

Table S1. Calculated values of ρ_{CM} and molar ratios of H_2O:D_2O

	ρ_{CM} (Å^{-2})	H_2O:D_2O at CM condition
h-/*d*-DPPC bicelle (Q=2.5)	1.97 x10^{-6}	0.635 : 0.365
h-/*d*-DPPC bicelle (Q=3)	2.04 x10^{-6}	0.624 : 0.376
h-/*d*-DPPC bicelle (Q=3.5)	2.10 x10^{-6}	0.616 : 0.384
PEGlyated *h*-/*d*-DMPC bicelle (Q=3)	1.91 x10^{-6}	0.643 : 0.357
PEGlyated h-/*d*-DPPC bicelle (Q=3)	1.96 x10^{-6}	0.636 : 0.364

S2 Time-Resolved Small Angle Neutron Scattering

S2.1. SANS Fitting Results

SANS data of bicellar mixtures were best fit using a polydisperse radius discoidal model, where the size averaged form factor $P_{disc}(q)$ and scattering amplitude $A_{disc}(q,\alpha)$ are expressed as:

$$P_{disc}(q) = \frac{1}{V_{disc}}\int_0^{\infty} f(r)dr \int_0^{\pi/2} A_{disc}{}^2(q,\alpha)sin\alpha d\alpha, \tag{S1}$$

$$A_{disc}(q,\alpha) = 2V_{disc}(\rho_{disc} - \rho_{CM})j_0(\frac{qt}{2}cos\alpha)\frac{J_1(qrsin\alpha)}{(qrsin\alpha)}, \tag{S2}$$

where V_{disc} is the average disc volume, *f(r)* is the Schulz distribution, α is the angle between the bilayer normal and the scattering vector, *q*, and *t* is the disc thickness. The polydispersity, *p*, of the bicelle radius, *r*, in the Schulz distribution function is defined as the ratio of the standard deviation, σ, of *r* to the average of *r*, $< R_i >$, i.e. $p = \frac{\sigma}{<R_i>}$. Then the Schultz distribution function can be expressed as:

$$f(r) = \frac{p^{-2/p^2}}{<R_i>\Gamma(1/p^2)}(\frac{r}{\langle R_i\rangle})^{\frac{(1-p^2)}{p^2}}\exp(-\frac{r}{p^2<R_i>}), \tag{S3}$$

where $\Gamma(x)$ is the Gamma function. The functions $J_1(x)$ and $j_0(x)$ are the first order Bessel and first spherical Bessel functions ($\frac{\sin(x)}{x}$), respectively. Eqn (S1) includes the average overall possible orientations and different size of discs. The average volume for the disc can be approximated as $V_{disc} = \pi r^2 t(\frac{z+2}{z+1})$, based on *r* following the Schulz distribution, and z is related to the polydispersity, p ($z = \frac{1}{p^2} - 1$). The radius and thickness of the bicelles used in the model were chosen based on the values obtained from the best fit to the data from the highest-contrast sample (i.e., the initial condition). The value of ρ_{CM} was also calculated based on the H_2O/D_2O composition. Therefore, the only variable parameter as a function of time is the NSLD of the bicelles, ρ_{disc}. Tables S2 to S4 summarize the best fit data of ρ_{disc} from the time-resolved SANS data of DPPC bicelles at different temperatures. The NSLD contrast ($\Delta\rho$) between CM solvent (ρ_s) and bicelles were then calculated at different times. The lipid transfer kinetics in bicelle can be characterized using a single exponential decay[1]

$$|\rho(t) - \rho_s| = \Delta\rho_0 e^{-kt} \quad \text{(S4)}$$

where $\Delta\rho_0$ is the SLD difference between the CM solvent and the bicelles at t = 0, and k is the apparent spontaneous lipid transfer rate constant.

Table S2. Best fit values of ρ_{disc} from time-resolved SANS data of Q = 3 *h-/d-* DPPC bicellar mixtures at 20 ºC, with a radius and thickness of 64 - 67 Å and 34.6 - 36.7 Å, respectively, and a fixed ρ_s of 2.04 x10^{-6} Å^{-2}.

	0.6 hrs	52 hrs	77 hrs	101 hrs	150 hrs
ρ_{disc} (Å^{-2})	4.94 x 10^{-6} or -8.6 x 10^{-7}	4.75 x 10^{-6} or -6.7 x10^{-7}	4.64 x 10^{-6} or -5.6 x 10^{-7}	4.58 x 10^{-6} or -5.0 x 10^{-7}	4.44 x 10^{-6} or -3.6 x 10^{-7}
$\Delta\rho$ (Å^{-2})	2.90 x 10^{-6} ± 9 x 10^{-9}	2.71 x 10^{-6} ± 6.2 x 10^{-8}	2.60 x 10^{-6} ± 5.1 x 10^{-8}	2.54 x 10^{-6} ± 6.2 x 10^{-8}	2.4 x 10^{-6} ± 1.04 x 10^{-7}
	199 hrs	**269 hrs**	**366 hrs**	**440 hrs**	**513 hrs**
ρ_{disc} (Å^{-2})	4.42 x 10^{-6} or -3.4 x 10^{-7}	4.18 x 10^{-6} or -1.0 x10^{-7}	4.03 x 10^{-6} or 5 x 10^{-8}	4.58 x 10^{-6} or 1.3 x 10^{-7}	3.82 x 10^{-6} or -2.6 x 10^{-7}
$\Delta\rho$ (Å^{-2})	2.38x 10^{-6} ± 9 x 10^{-9}	2.14 x 10^{-6} ± 6.2 x 10^{-8}	1.99 x 10^{-6} ± 5.1 x 10^{-8}	1.91 x 10^{-6} ± 6.2 x 10^{-8}	1.78 x 10^{-6} ± 1.04 x 10^{-7}

Table S3. Best fit values of ρ_{disc} from time-resolved SANS data of Q = 3 *h-/d-* DPPC bicellar mixtures at 25 ºC, with a radius and thickness of 65 - 69 Å and 31 - 36 Å, respectively, and a fixed ρ_s of 2.04 x10^{-6} Å^{-2}.

	0.45 hrs	11 hrs	16 hrs	26 hrs	42 hrs
ρ_{disc} (Å^{-2})	4.95 x 10^{-6} or -8.7 x 10^{-7}	4.86 x 10^{-6} or -7.8 x10^{-7}	4.82 x 10^{-6} or -7.4 x 10^{-7}	4.75 x 10^{-6} or -6.7 x 10^{-7}	4.61 x 10^{-6} or -5.3 x 10^{-7}
$\Delta\rho$ (Å^{-2})	2.91 x 10^{-6} ± 3.65 x 10^{-9}	2.82 x 10^{-6} ± 3.32 x 10^{-9}	2.78 x 10^{-6} ± 4.21 x 10^{-9}	2.71 x 10^{-6} ± 3.46 x 10^{-8}	2.57 x 10^{-6} ± 5.17 x 10^{-9}
	50 hrs	56 hrs	82 hrs	108 hrs	159 hrs
ρ_{disc} (Å^{-2})	4.56 x 10^{-6} or -4.8 x 10^{-7}	4.49 x 10^{-6} or -4.1 x10^{-7}	4.35 x 10^{-6} or -2.7 x 10^{-7}	4.17 x 10^{-6} or -9 x 10^{-8}	3.98 x 10^{-6} or 1.0 x 10^{-7}
$\Delta\rho$ (Å^{-2})	2.52x 10^{-6} ± 3.69 x 10^{-9}	2.45 x 10^{-6} ± 3.76 x 10^{-9}	2.31 x 10^{-6} ± 3.77 x 10^{-9}	2.13 x 10^{-6} ± 2.71 x 10^{-9}	1.94 x 10^{-6} ± 3.18 x 10^{-9}
	184 hrs	233 hrs	259 hrs	356 hrs	407 hrs
ρ_{disc} (Å^{-2})	3.78 x 10^{-6} or 3.0 x 10^{-7}	3.71 x 10^{-6} or 3.7 x10^{-7}	3.62 x 10^{-6} or 4.6 x 10^{-7}	3.39 x 10^{-6} or 6.9 x 10^{-7}	3.20 x 10^{-6} or -8.8 x 10^{-7}
$\Delta\rho$ (Å^{-2})	1.74 x 10^{-6} ± 3.40 x 10^{-9}	1.67 x 10^{-6} ± 3.58 x 10^{-9}	1.58 x 10^{-6} ± 4.28 x 10^{-9}	1.35 x 10^{-6} ± 5.01 x 10^{-9}	1.16 x 10^{-6} ± 1.21 x 10^{-9}

Table S4. Best fit values of ρ_{disc} from time-resolved SANS data of Q = 3 h-/d- DPPC bicellar mixtures at 30 ºC, with a radius and thickness of 66 - 70 Å and 32 - 36 Å, respectively, and a fixed ρ_s of 2.04 x10^{-6} Å^{-2}.

	0.4 hrs	7 hrs	12 hrs	14 hrs	23 hrs
ρ_{disc} (Å^{-2})	4.98 x 10^{-6} or -9.0 x 10^{-7}	4.83 x 10^{-6} or -7.5 x10^{-7}	4.74 x 10^{-6} or -6.6 x 10^{-7}	4.73 x 10^{-6} or -6.5 x 10^{-7}	4.56 x 10^{-6} or -4.8 x 10^{-7}
$\Delta\rho$ (Å^{-2})	2.94 x 10^{-6} ± 3.73 x 10^{-9}	2.79 x 10^{-6} ± 3.61 x 10^{-9}	2.70 x 10^{-6} ± 3.51 x 10^{-9}	2.69 x 10^{-6} ± 3.84 x 10^{-9}	2.52 x 10^{-6} ± 4.95 x 10^{-9}
	34 hrs	60 hrs	85 hrs	109 hrs	146 hrs
ρ_{disc} (Å^{-2})	4.34 x 10^{-6} or -2.6 x 10^{-7}	3.79 x 10^{-6} or 2.9 x10^{-7}	3.53 x 10^{-6} or -5.5 x 10^{-7}	3.4 x 10^{-6} or 6.8 x 10^{-7}	3.37 x 10^{-6} or 7.1 x 10^{-7}
$\Delta\rho$ (Å^{-2})	2.30x 10^{-6} ± 7.62 x 10^{-9}	1.75 x 10^{-6} ± 3.81 x 10^{-9}	1.49 x 10^{-6} ± 3.85 x 10^{-9}	1.36 x 10^{-6} ± 7.27 x 10^{-9}	1.33 x 10^{-6} ± 4.45 x 10^{-9}
	184 hrs	233 hrs	283 hrs		
ρ_{disc} (Å^{-2})	3.11 x 10^{-6} or 9.7 x 10^{-7}	3.07 x 10^{-6} or 1.01 x10^{-6}	2.99 x 10^{-6} or 1.09 x 10^{-7}		
$\Delta\rho$ (Å^{-2})	1.07 x 10^{-6} ± 2.06 x 10^{-8}	1.03 x 10^{-6} ± 7.15 x 10^{-9}	9.52 x 10^{-7} ± 2.87 x 10^{-8}		

S3 Time-Resolved Differential Scanning Calorimetry

S3.1. TR-DSC data

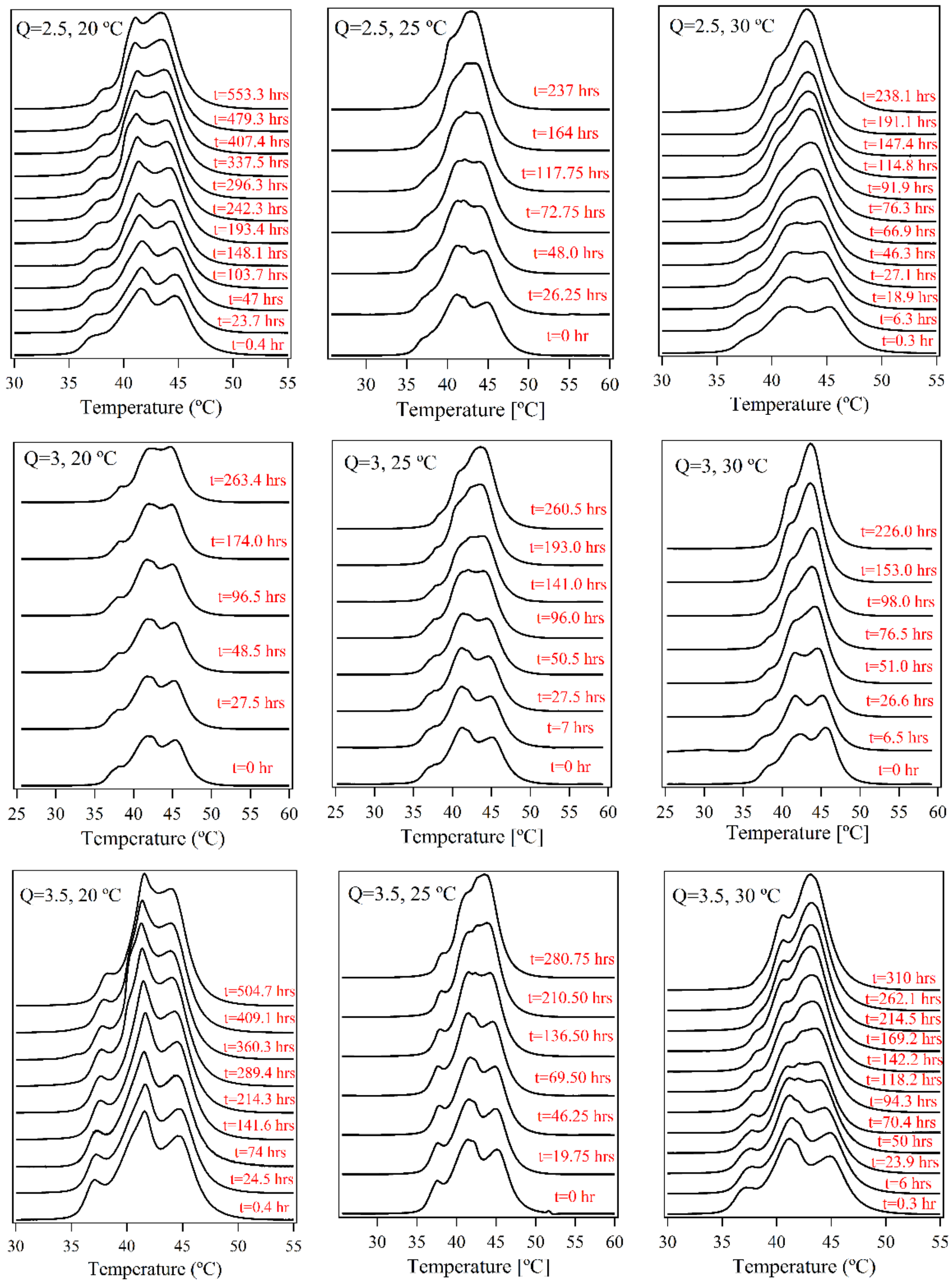

Figure S1 TR-DSC data of lipid transfer between bicelles of different *Q* values.

Figure S1 shows the TR-DSC data collected for lipid transfer experiments of different *Q*. The two distinct peaks are clearly visible in each DSC endotherm at early mixing periods, corresponding to the melting transition of *d*- bicelles (lower T_M) and *h*- bicelles (higher T_M). As the lipid transfer between *h*- and *d*- bicelles takes place, these peaks move toward each other. the DSC endotherm contains other minor peaks, possibly due to the presence of *d*- and *h*- vesicles with increasing *T*.[2] The difference in T_M between bicelles and vesicles of the same molecular make up is presumably due to their distinct cooperative units.[3, 4] All the T_Ms, including those of *d*- and *h*- bicelles and vesicles, were identified using a sum of four independent Gaussian curves. ΔT_M between *h*-rich and *d*-rich bicelles can then be calculated at each *t* using the lipid transfer rate equation (S5)

$$T_{M,h} - T_{M,d} = \Delta T_{M,o} e^{-kt} \tag{S5}$$

where $T_{M,h}$ and $T_{M,d}$ is the T_M of *h*-rich and *d*-rich bicelles, respectively. $\Delta T_{M,o}$ is the initial ΔT_M ($T_{M,h} - T_{M,d}$) at $t = 0$.

S3.2. Gaussian Fitting Results

DSC scans were fit using four Gaussians (*d*- an *h*- DPPC associated with bicelles and vesicles are shown in Tables S5-S13).

Table S5. DSC peak positions obtained by Gaussian fits of Q = 2.5 DPPC bicelles at 20 ºC and as a function of time

	d-vesicle	*d*-bicelle	*h*-vesicle	*h*-bicelle	$\Delta T_{bicelle}$
0.4 hr	37.44±0.18	40.32±0.35	41.74±0.08	44.45±0.03	4.13±0.38
24 hrs	37.50±0.05	40.71±0.16	41.81±0.08	44.55±0.05	3.84±0.20
47 hrs	37.84±0.18	40.62±0.39	41.88±0.10	44.41±0.03	3.79±0.42
104 hrs	37.81±0.11	40.61±0.37	41.66±0.06	44.08±0.06	3.47±0.43
148 hrs	37.76±0.06	40.70±0.33	41.60±0.06	44.07±0.06	3.37±0.38
193 hrs	38.04±0.18	40.64±1.18	41.54±0.26	43.84±0.06	3.21±1.24
338 hrs	38.08±0.08	41.08±0.10	40.75±0.03	43.45±0.03	2.70±0.06

Table S6. DSC peak positions obtained by Gaussian fits of Q = 2.5 DPPC bicelles at 25 ºC and as a function of time

	d-vesicle	*d*-bicelle	*h*-vesicle	*h*-bicelle	$\Delta T_{bicelle}$
0 hr	37.95±0.19	40.78±0.13	42.15±0.07	44.61±0.04	3.832±0.17
26.5 hrs	38.35±0.19	40.88±0.07	42.16±0.07	44.11±0.05	3.23±0.12
48 hrs	38.30±0.15	40.79±0.03	42.17±0.05	43.80±0.04	3.01±0.07
72.8 hrs	38.57±0.18	40.89±0.06	42.22±0.06	43.72±0.04	2.83±0.09

Table S7. DSC peak positions obtained by Gaussian fits of Q = 2.5 DPPC bicelles at 30 ºC and as a function of time

	d-vesicle	*d*-bicelle	*h*-vesicle	*h*-bicelle	$\Delta T_{bicelle}$
0.3 hr	38.25±0.29	40.92±0.19	42.44±0.14	44.98±0.27	4.06±0.22
6.3 hrs	38.17±0.40	40.75±0.56	42.11±0.29	44.59±0.35	3.84±0.59
18.9 hrs	38.61±0.37	40.99±0.87	42.07±0.38	44.24±0.05	3.25±0.92
27.1 hrs	38.80±0.30	41.01±0.41	42.09±0.32	43.95±0.04	2.94±0.45
46.3 hrs	37.94±0.02	41.52±0.02	42.88±0.03	44.23±0.02	2.71±0.04

Table S8. DSC peak positions obtained by Gaussian fits of Q = 3.0 DPPC bicelles at 20 ºC and as a function of time

	d-vesicle	*d*-bicelle	*h*-vesicle	*h*-bicelle	$\Delta T_{bicelle}$
0 hr	37.99±0.16	40.90±0.31	42.42±0.12	45.13±0.03	4.23±0.34
27.5 hrs	38.99±0.16	41.00±0.42	42.33±0.13	44.98±0.04	3.98±0.46
48.4 hrs	38.13±0.16	41.06±0.36	42.41±0.15	44.96±0.03	3.90±0.39
96.5 hrs	38.17±0.15	41.10±0.34	42.34±0.16	44.70±0.04	3.61±0.38
174 hrs	38.45±0.06	41.20±0.40	42.36±0.22	44.61±0.04	3.41±0.44
263 hrs	38.66±0.15	41.26±0.22	42.51±0.21	44.48±0.03	3.21±0.25

Table S9. DSC peak positions obtained by Gaussian fits of Q = 3.0 DPPC bicelles at 25 ºC and as a function of time

	d-vesicle	*d*-bicelle	*h*-vesicle	*h*-bicelle	$\Delta T_{bicelle}$
0 hr	37.50±0.15	40.66±0.65	41.94±0.20	44.80±0.06	4.14±0.71
7 hrs	37.52±0.21	40.53±0.68	41.83±0.31	44.57±0.04	4.05±0.72
27 hrs	37.75±0.11	40.78±0.12	42.10±0.08	44.36±0.04	3.59±0.16
50.5 hrs	37.98±0.12	40.84±0.08	42.21±0.08	44.20±0.03	3.36±0.11
96 hrs	37.68±0.12	41.29±0.06	42.61±0.08	44.24±0.03	3.10±0.11

Table S10. DSC peak positions obtained by Gaussian fits of Q = 3.0 DPPC bicelles at 30 ºC and as a function of time

	d-vesicle	*d*-bicelle	*h*-vesicle	*h*-bicelle	$\Delta T_{bicelle}$
0 hr	38.41±0.25	41.23±0.31	42.77±0.15	45.47±0.02	4.24±0.33
6.5 hrs	37.64±0.06	39.11±0.20	41.46±0.03	45.14±0.04	3.67±0.24
26.7 hrs	38.68±0.12	41.33±0.03	N/A	44.36±0.03	3.03±0.06

Table S11. DSC peak positions obtained by Gaussian fits of Q = 3.5 DPPC bicelles at 20 ºC and as a function of time

	d-vesicle	*d*-bicelle	*h*-vesicle	*h*-bicelle	$\Delta T_{bicelle}$
0.4 hr	37.11±0.04	40.28±0.16	41.67±0.02	44.43±0.04	4.15±0.21
24.5 hrs	37.25±0.05	40.32±0.21	41.72±0.02	44.44±0.04	4.12±0.25
74 hrs	37.29±0.07	40.18±0.32	41.57±0.04	44.20±0.05	4.02±0.36
141.6 hrs	37.62±0.09	40.30±0.29	41.69±0.05	44.21±0.02	3.91±0.32
214.3 hrs	37.60±0.05	40.27±0.07	41.52±0.02	43.96±0.05	3.70±0.12

Table S12. DSC peak positions obtained by Gaussian fits of Q = 3.5 DPPC bicelles at 25 ºC and as a function of time

	d-vesicle	*d*-bicelle	*h*-vesicle	*h*-bicelle	$\Delta T_{bicelle}$
0 hr	37.54±0.08	40.66±0.32	42.12±0.09	44.92±0.04	4.26±0.36
19.8 hrs	37.64±0.10	40.67±0.47	42.07±0.13	44.76±0.04	4.09±0.51
46.3 hrs	37.84±0.11	40.74±0.62	42.09±0.17	44.62±0.04	3.88±0.66
69.5 hrs	37.73±0.13	40.65±1.34	41.81±0.33	44.32±0.07	3.68±1.41
136.5 hrs	37.91±0.01	41.40±0.02	42.97±0.08	44.38±0.02	2.98±0.04
210.5 hrs	38.20±0.05	40.85±0.02	42.43±0.06	43.66±0.03	2.81±0.05

Table S13. DSC peak positions obtained by Gaussian fits of Q = 3.5 DPPC bicelles at 30 ºC and as a function of time

	d-vesicle	*d*-bicelle	*h*-vesicle	*h*-bicelle	$\Delta T_{bicelle}$
0.3 hr	37.13±0.07	40.26±0.89	41.53±0.12	44.64±0.06	4.38±0.94
6.0 hrs	37.55±0.10	40.57±0.84	41.78±0.15	44.65±0.06	4.08±0.90
23.9 hrs	37.52±0.17	40.45±2.17	41.52±0.69	44.12±0.02	3.67±2.19
50.0 hrs	37.80±0.05	40.71±0.02	42.14±0.05	43.67±0.03	2.95±0.05
70.4 hrs	37.76±0.03	40.65±0.02	42.12±0.03	43.49±0.01	2.84±0.02
94.3 hrs	38.10±0.07	40.51±0.03	42.15±0.05	43.29±0.03	2.78±0.06

S4 Determination of the Morphology of Different-Q Bicelles Using SANS

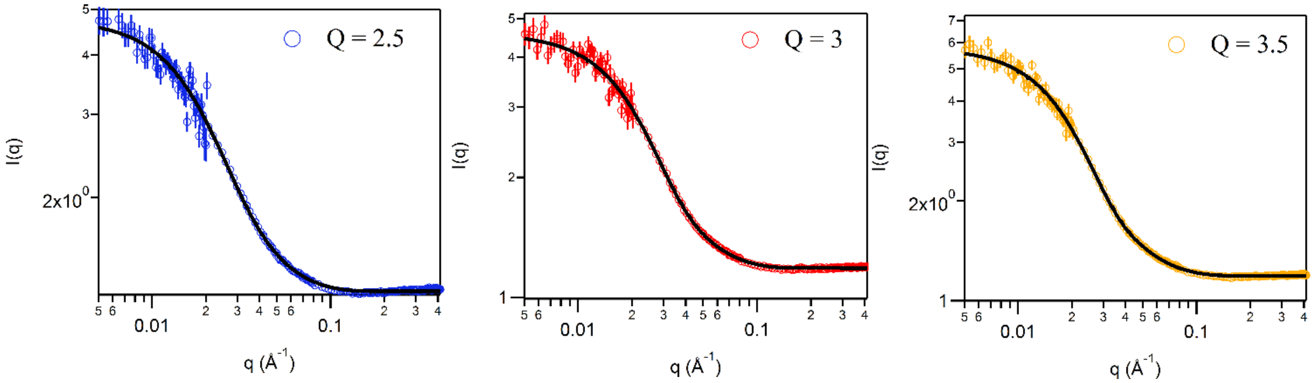

Figure S2. SANS data of initial DPPC/DPPG/DHPC bicelles with different Q values and constant charged lipid ratio R = 0.05 at 10 °C at initial stage of lipid transfer.

SANS measurements were conducted at NCNR to determine the bicelle size at different Qs. Fig. S2 shows examples of SANS data of different Q (2.5, 3.0 and 3.5) DPPC bicelles. The solid lines are the best fits to the data using a discoidal model, as described in S2. Although there is a strong charge effect, the structure factor did not appear in the SANS curves because of the contrast-matched condition. We were therefore able to fit the data using only the discoidal form factor. Table S14 lists the best fit parameters, indicating that bicelle radii decrease with increased amounts of DHPC (i.e., increased fraction of interface in a bicelle). This is the most likely explanation for the observed enhanced lipid transfer rate constants observed as a function of increased amounts of DHPC.

TABLE S14. Best fit parameters from SANS data of DPPC bicelles

	Radius (Å)	Thickness (Å)
Q = 2.5	73.2 ± 0.8	38.0 ± 0.4
Q = 3.0	81.7 ± 0.7	38.8 ± 0.4
Q = 3.5	95.0 ± 0.6	38.3 ± 0.4

S5 DSC Endotherms of h-, d- and h-/d- Bicelles

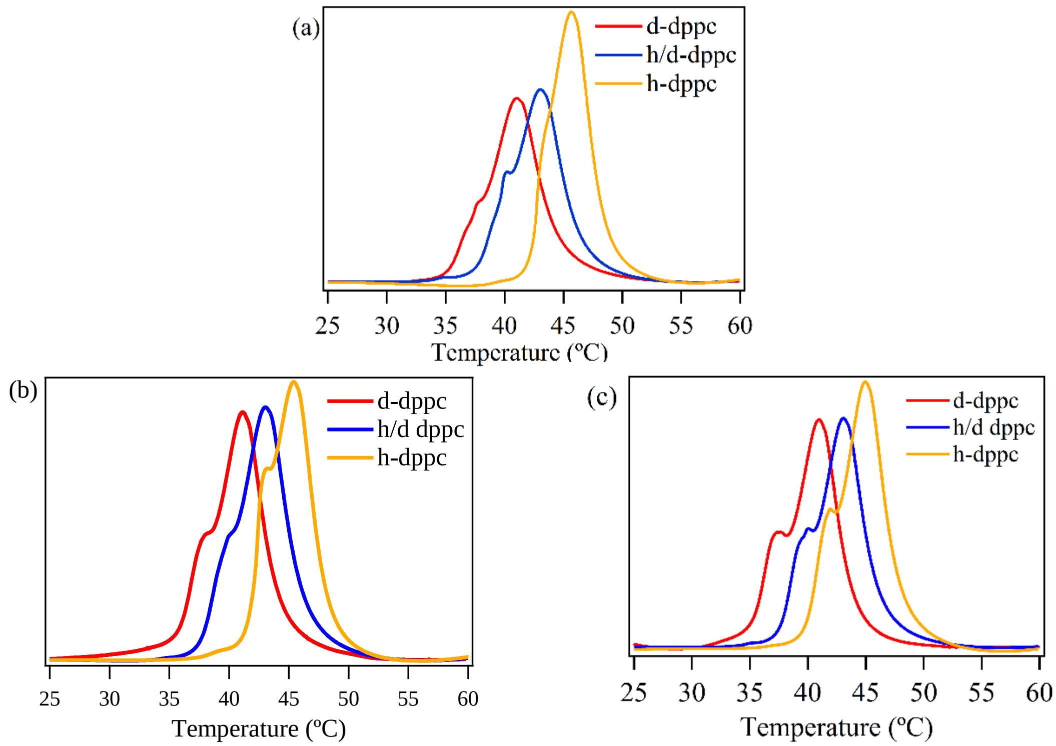

Figure S3. DSC data of Q = 2.5 (a), 3 (b) and 3.5 (c) *h*-, *h/d*- and *d*- DPPC bicelles.

S5.1. DSC data of pure h-, d- and intimate mixed equal molar h-/d- DPPC bicelles

Fig S2 shows DSC scans of *h*-, *h/d*- and *d*-DPPC bicelles, where *h/d*-DPPC bicelles were prepared through mixing equal molar deuterated and protiated DPPC lipids. Each curve has a major peak and a shoulder, most likely corresponding to the T_M of DPPC associated with vesicles, whose T_M is known to be lower than that of bicelles. Table S14 shows that the T_M difference (ΔT_M) between *h*-bicelles and *d*-bicelles is ~ 4ºC, providing sufficient separation to differentiate between peaks. The T_M for *h/d* bicelles is similar to the average of $T_{M,h}$ and $T_{M,d.}$

Table S15. T_M summary of DPPC bicelles

	Q = 2.5	Q = 3	Q = 3.5
$T_{M,h}$	45.66	45.42	44.99
$T_{M,d}$	41.03	41.13	40.98
$T_{M,h/d}$	43.02	43.03	43.07
ΔT_M	4.63	4.19	4.01

S5.2. Phase Transition Enthalpy

In order to compare phase transition enthalpies at different Q values, we integrated each phase transition peak to obtain the phase transition enthalpy (ΔH_{fu}), summarized in Table S16. It should be noted that the transition enthalpy was normalized based on the amounts of DPPC and DPPG, and not DHPC, since DHPC does not undergo a phase transition over the temperature range studied. It was found that ΔH is smallest for Q = 2.5. The decrease in ΔH is most likely the result of increased DPPC/DHPC fraction at the interfacial region between domains, allowing DPPC to melt from the gel to the liquid crystalline phase at lower energy cost. This interface between domains is thought to enhance the transfer rate of DPPC.

Table S16. Phase transition enthalpies of DPPC bicelles ($\Delta H_{fu,h}$, $\Delta H_{fu,d}$ and $\Delta H_{fu,h/d}$ are the enthalpies for *h*-, *d*- and *h/d*- bicelles, respectively.)

	Q = 2.5	Q = 3	Q = 3.5
$\Delta H_{fu,h}$	16.18	18.54	19.54
$\Delta H_{fu,d}$	14.84	19.87	18.64
$\Delta H_{fu,h/d}$	15.3	19.2	18.51

S6 Lipid Exchange between PEGylated Bicelles

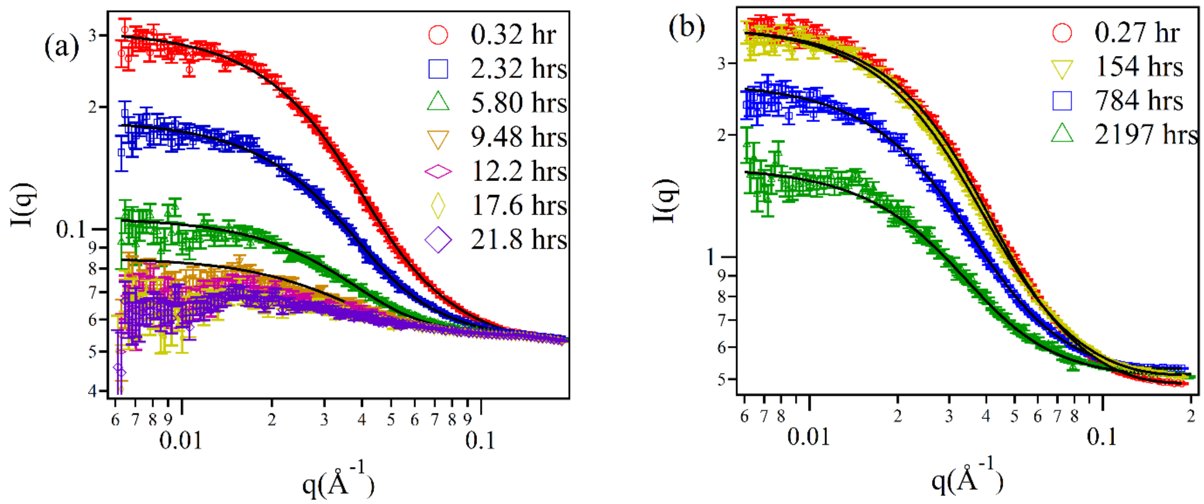

Figure S4. TR-SANS data of the lipid transfer on the PEGylated bicelles at 10 °C. (a) DMPC/DMPG/DHPC/DSPE-PEG2000, Q = 3, R = 0.05, and DSPE-PEG2000 ratio of 5.0 mol.% (b) DPPC/DPPG/DHPC/DSPE-PEG2000, Q = 3, R = 0.05, and DSPE-PEG2000 ratio of 5.0 mol.%. The solid lines are the best fits using a disk model with polydispersed radii to generate the neutron scattering length density (NSLD) of bicelle.

Tables S17 and S18 tabulate the best fit parameters for DMPC and DPPC bicelles containing DSPE-PEG2000.

Table S17. Best fit results from SANS data of DMPC/DMPG/DHPC/PEG2000-DSPE bicelles at 10 ^{o}C with a radius of ~ 58 Å, a thickness of ~ 29 Å, and a fixed ρ_s of 1.91 x10^{-6} Å^{-2}.

	0.32 hrs	2.32 hrs	5.80 hrs	9.48 hrs
ρ_{disc} (Å^{-2})	2.69 x 10^{-6} or 1.13 x 10^{-6}	2.48 x 10^{-6} or 1.34 x10^{-6}	2.29 x 10^{-6} or 1.53 x 10^{-7}	2.20 x 10^{-6} or 1.62 x 10^{-7}
$\Delta\rho$ (Å^{-2})	7.79 x 10^{-7} ± 4.28 x 10^{-9}	5.70 x 10^{-7} ± 5.93 x 10^{-10}	3.77 x 10^{-6} ± 7.31 x 10^{-10}	2.86 x 10^{-7} ± 9.16 x 10^{-10}

TABLE S18. Best fit results from SANS data of DPPC/DPPG/DHPC/PEG2000-DSPE bicelles at 10 ^{o}C with a radius of ~ 57 Å, a thickness of ~ 33 Å, and a fixed ρ_s of 1.96 x10^{-6} Å^{-2}.

	0.27 hrs	1.54 hrs	784 hrs	2197 hrs
ρ_{disc} (Å^{-2})	4.54 x 10^{-6} or -6.2 x 10^{-7}	4.41 x 10^{-6} or -4.9 x10^{-7}	4.25 x 10^{-6} or -3.3 x 10^{-7}	4.16 x 10^{-6} or 5.2 x 10^{-7}
$\Delta\rho$ (Å^{-2})	2.58 x 10^{-6} ± 8.58 x 10^{-9}	2.45 x 10^{-6} ± 8.20 x 10^{-9}	1.88 x 10^{-6} ± 7.32 x 10^{-9}	1.44 x 10^{-6} ± 2.67 x 10^{-9}

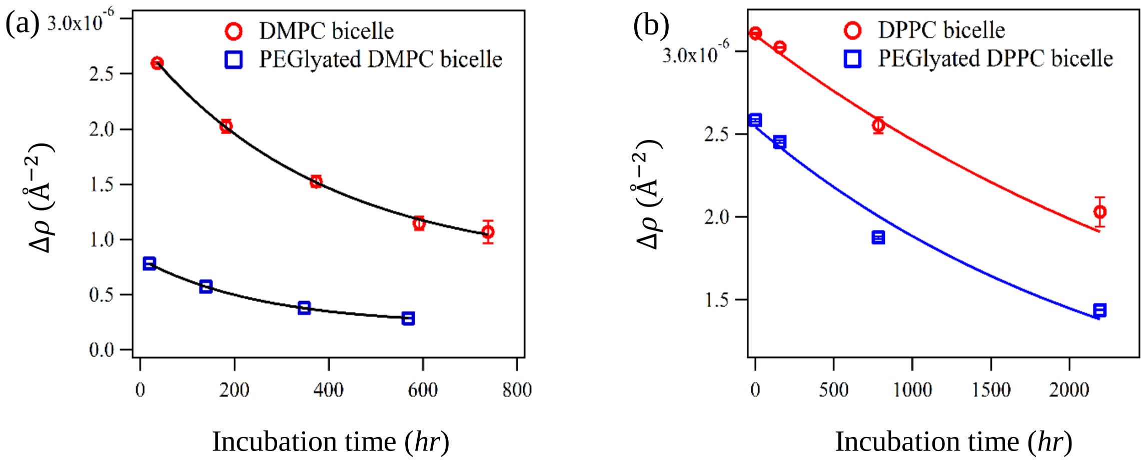

Figure. S5. The time evolution NSLD contrast, $\Delta\rho$ of (a) DMPC/DMPG/DHPC and (b) DPPC/DPPG/DHPC bicelles in the absence and presence of DSPE-PEG2000. The solid lines are the best fits using eq (S4). The non-PEGlyated bicelle data were obtained from previous report.[1]

The derived values for k_{inter} are $(4.13 \pm 0.15) \times 10^{-4}$ and 0.233 ± 0.003 hr^{-1} for 10 ^{o}C DSPE-PEG2000-associated DPPC and DMPC bicelles, respectively.

References

1. Xia, Y.; Li, M.; Charubin, K.; Liu, Y.; Heberle, F. A.; Katsaras, J.; Jing, B.; Zhu, Y.; Nieh, M. P. Effects of Nanoparticle Morphology and Acyl Chain Length on Spontaneous Lipid Transfer Rates. *Langmuir* **2015,** *31* (47), 12920-8.
2. Denisov, I. G.; McLean, M. A.; Shaw, A. W.; Grinkova, Y. V.; Sligar, S. G. Thermotropic phase transition in soluble nanoscale lipid bilayers. *J Phys Chem B* **2005,** *109* (32), 15580-8.
3. Marsh, D.; Watts, A.; Knowles, P. F. Cooperativity of the phase transition in single- and multibilayer lipid vesicles. *Biochim Biophys Acta* **1977,** *465* (3), 500-14.
4. Shaw, A. W.; McLean, M. A.; Sligar, S. G. Phospholipid phase transitions in homogeneous nanometer scale bilayer discs. *FEBS Lett* **2004,** *556* (1-3), 260-4.